doi: 10.31674/book.2024ecc.001

# A New Ratiometric Highly Selective Chromogenic Sensor for $Cu^{2+}$ Detection

**Puspendu Roy**

*Department of Chemistry, Netaji Nagar Day College, Kolkata, West Bengal, India*

*Corresponding Author's Email: roypuspendu1991@gmail.com*

**Abstract:**

An azo-phenol moiety-based chemosensor is synthesized and different spectroscopic techniques have been used to confirm its structure. A significant colour change from pale yellow to purple was noticed while the chemosensor made a complex with $Cu^{2+}$ ion but it did not show any significant colour change while studied with other competitive metal ions. Job's plot and mass spectroscopic analysis have been used to predict the 1:1 chemosensor-$Cu^{2+}$ complex formation. DFT studies have been performed to explain the binding mechanism between the HL and $Cu^{2+}$.Association constant (Ka, $8.94x10^4$ $M^{-1}$) confirms that the probe has very high affinity for $Cu^{2+}$ complex formation. Thus, the probe is highly effective in comparison to other reported probes for selective colorimetric and ratiometric detection of $Cu^{2+}$.

***Keywords:*** *Azo Phenol Moiety Based Chemosensor; Colorimetric and Ratiometric $Cu^{2+}$ Sensor; DFT Computational Studies*

## Introduction:

As copper is required in almost every living organism (Kim, Nevitt & Thiele, 2008), it is employed as a catalyst in several biological methods such as hormone maturation, oxygen transportation and signal transduction (Robinson & Winge, 2010). In human body, $Cu^{2+}$ is the third most abundant essential trace element and it has an important role in many physiological methods (Chang, 2023; Linder & Hazegh-Azam, 1996). The concentration of $Cu^{2+}$ ion in environmental sample has to be monitored to prevent the effect of disorder in Cu (II) metabolism by severe neurodegenerative diseases, such as Alzheimer's and Wilson's diseases (Finkel, Serrano & Blasco, 2007; Zou *et al*., 2012; Guo, Chen & Duan, 2010; Dalapati *et al*., 2011, Vulpe *et al*., 1993; Hahn *et al*., 1995).

Colorimetric sensors are in high demand due to the simple visualization of color by the naked eye and also for its simple and rapid implementation (Veedu *et al*., 2024; Elmagbari *et al*., 2024; Trevino *et al*., 2023; Cao *et al*., 2022; Chen *et al*., 2010; Shang, Zhang & Dong, 2009; Ajayakumar *et al*., 2010). So, the synthesis of chemosensor for the detection of $Cu^{2+}$, especially selective ratiometric detection, is in high demand.

In this present work, the synthetic method and photo-physical properties of ONS linkage containing azo phenol moiety-based ligand has been described, which shows a significant colour change from light yellow to pink upon complexation with $Cu^{2+}$ because of the increase in ICT (internal charge transfer). Several spectroscopic studies prove that the chemosensor exhibits a very good affinity for $Cu^{2+}$ in acetonitrile solvent.

### *Synthesis of azo phenol moiety based ligand (HL)*

3.06 g of 2-(ethylthio)benzenamine was dissolved in 10 mL of 1:1 HCl solution and then the solution was cooled by keeping it in an ice bath. 2.0 g $NaNO_2$ in 10 mL water was poured into it in ice cold condition under stirring. Then the mixture of solution was added to 25 mL of 6 g solution of $Na_2CO_3$ under ice cold condition and 2.56 g of 4-chlorophenol was added under vigorous stirring codition. An orange-red precipitate was filtered off and the precipitate was washed with cold water and then dried. Column chromatography technique was used for the further purification of the product by using 35% (v/v) ethyl acetate-petroleum ether mixture.

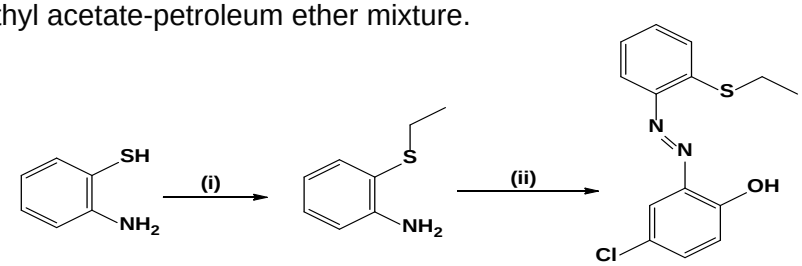


**Scheme 1**: Synthetic route of ligand ((i) Na in dry MeOH, (ii) $NaNO_2$, dil. HCl, 4-chloro phenol in $Na_2CO_3$ (0-5$^0$C)

### Synthesis of $Cu^{2+}$ complex

Ligand (HL) was dissolved in acetonitrile solvent and $CuCl_2.H_2O$ was added to it under stirring condition for 3 hours. The residue was filtered and washed with hexane. The obtained yield was 0.094 g ( 78.2%).

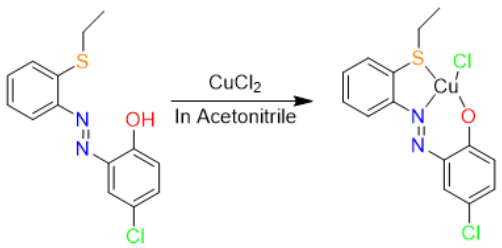


### UV-Vis titration method

10 μM stock solution of the chemosensor ligand (HL) was prepared in $CH_3CN$. 10 μM of Chloride salts of the each guest cations were also prepared in $CH_3CN$. Various

concentrations of chemosensor ligand (host) were also taken and increasing concentrations of guest cations were used separately. The sharp changes in UV-Vis spectra of chemosensor ligand (host) upon gradual addition of the guest cations solutions were studied.

**Job's plot (absorbance method)**

A series of 10 μM solutions of HL and $CuCl_2$ were prepared for the Job's plot by maintaining the total volume of the metal ion and HL remained constant (4 ml) in $CH_3CN$. In the Job's plots ΔA versus mole fraction of $Cu^{2+}$ was plotted. (ΔA = intensity change of the absorption spectrum at 515 nm).

**DFT Computational method**

Gaussian09 program has been used for DFT computations (Frisch, 2009). B3LYP was used for the geometrical optimization of the Cu complex (Beck, 1993; Lee, Yang & Parr, 1988). For C, H, N and O atoms 6-31+G(d) basis set was employed. The LANL2DZ basis set with effective core potential has been assigned for the Cu atom (Hay & Wadt, 1985; Wadt & Hay, 1985; Furche & Ahlrichs, 2002; Scalmani *et al*., 2006). The calculations based on vibrational frequency predict that the optimized structures represent the local minima of potential energy surface with only positive eigen-values. The time-dependent density functional theory (TDDFT) (Bauernschmitt & Ahlrichs, 1996; Stratmann, Scuseria & Frisch, 1998) in DMSO solvent has been used to predict singlet-singlet vertical electronic excitations. Conductor-like polarizable continuum model (CPCM) (Barone & Cossi, 1998; Cossi *et al*., 2003) has been employed for B3LYP optimized geometries.

**Cation sensing studies of HL by UV-Vis titration**

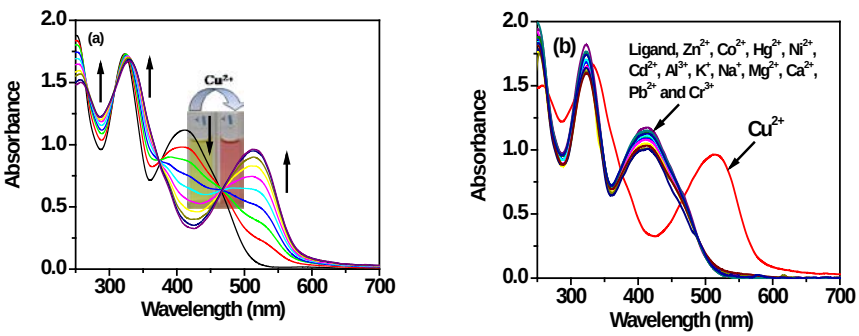


**Figure 1:** UV-vis titrimetric spectra of HL in presence of (i) $Cu^{2+}$ (0–1.5 equivalents) and (ii) different cations (3 equivalents). *(Source: Roy et al., 2017)*

An absorption spectra of the chemosensor ligand upon gradual addition of increasing concentrations of $Cu^{2+}$ (0–1.5 equiv) is shown in Figure 1. The spectra of ligand (Probe) shows two prominent absorbance peak at 323 nm and 410 nm in absence of any guest cation analytes. The absence of peak at 515 nm denotes that the probe is stable in this situation. A significant change in the absorbance spectra was observed after addition of $Cu^{2+}$. To obtain clear colorimetric change the solution of HL (10 µM) and the solution of $Cu^{2+}$ in acetonitrile have been prepared. The absorption band gradually decreases at 410 nm and a new band appears at 515 nm which gradually increases while incremental concentrations of $Cu^{2+}$ were used and a prominent isobestic point at 466 nm was observed.

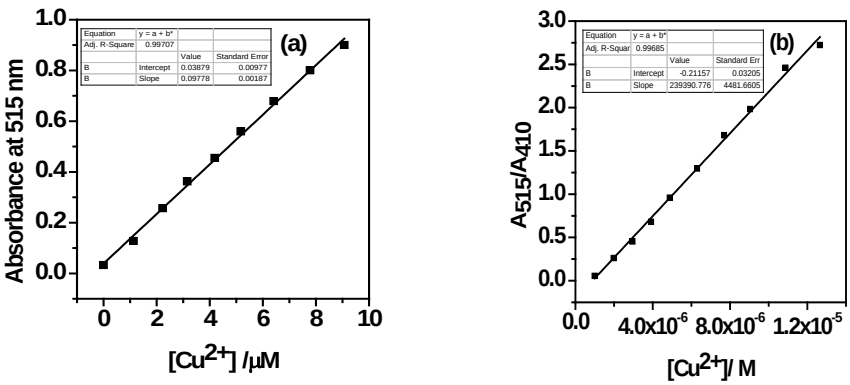


**Figure 2**: (a) Linear absorbance curve at 515 nm and (b) absorbance intensity ratio at $A_{515}/A_{410}$ nm of HL depending on the $Cu^{2+}$ concentration *(Source: Roy et al., 2017)*

A significant and clear color change of the stock solution from faint yellow to purple was observed by the photophysical changes. The large red shift (105 nm) of the absorption spectra of chemosensor receptor was noticed as ICT mechanism enhanced while the receptor made a complex with $Cu^{2+}$ ion. The absorbance profile of HL maintains a beautiful linear relationship with added $Cu^{2+}$ concentration (SI). The absorbance profile at 515 nm also maintains very good linearity when plotted against $Cu^{2+}$ concentration, as $R^2$ value is closer to 1. The limit of detection of the chemosensor for $Cu^{2+}$ is calculated from the absorption spectral change by taking the $Cu^{2+}$ concentration of $6.26 \times 10^{-8}$ M and by using the equation DL = K Sb1/S, where the value of K is taken as 3, Sb1 denotes the standard deviation of the blank solution, and S denotes the slope of the calibration curve. Absorption intensity band at 410 nm decreases and a ratiometric increase in the absorption intensity band at 515 nm is observed after gradual incremental addition of $Cu^{2+}$ solution. Saturation of intensity band is observed after the addition of a 1.0 equivalent of 10 µM solution of $Cu^{2+}$ ions shown in Fig. 1.

The novelty of any chemosensor probe can be determined by two very important parameters called interference and selectivity. The selectivity and sensitivity of the chemosensor towards $Cu^{2+}$ were examined by employing several guest cations ($Cd^{2+}$, $Co^{2+}$, $Cr^{3+}$, $Fe^{3+}$, $Hg^{2+}$, $K^{+}$ , $Mg^{2+}$, $Na^{+}$ , $Mn^{2+}$, $Ni^{2+}$, $Al^{3+}$, $Pb^{2+}$, $In^{3+}$ and $Zn^{2+}$). No significant change was observed in the absorbance spectra while other guest ions (except $Cu^{2+}$) were added. After the addition of $Cu^{2+}$, the absorbance of the chemosensor at 515 nm was increased by 27-fold. This phenomenon proves that the chemosensor can conveniently detect $Cu^{2+}$ ion by simple naked-eye inspection.

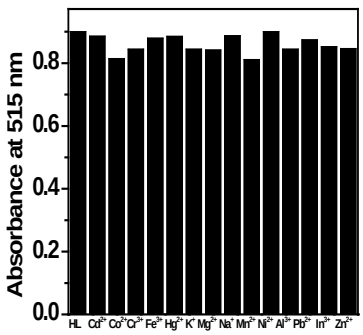


**Figure 3:** Competition study of several guest analytes(30 μM) using UV-vis method in the solution of probe(10 μM) in presence of $Cu^{2+}$ (20 μM). *(Source: Roy et al., 2017)*

***Job's plot***

By using same concentration (in the order of 10 μM in $CH_3CN$ at 25 °C) of chemosensor ligand and $Cu^{2+}$, the stock solution was prepared. Different sets of equal volume of chemosenor ligand-guest cations solution was prepared and the emission spectrum in each case was recorded. In the Job's plot ΔI.Xhost was taken as Y axis and Xhost was taken as X axis (ΔI = change in intensity of the absorbance spectrum at 515 nm and Xhost = the mole fraction of the ligand). It is evident from the Job's plot titration that the stoichiometry between probe and $Cu^{2+}$ is 1:1.

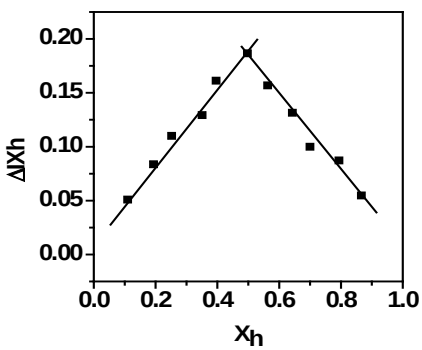


**Figure 4:** Job's plot of the prober for $Cu^{2+}$ Study of complexation mode (*Source: Roy et al., 2017)*

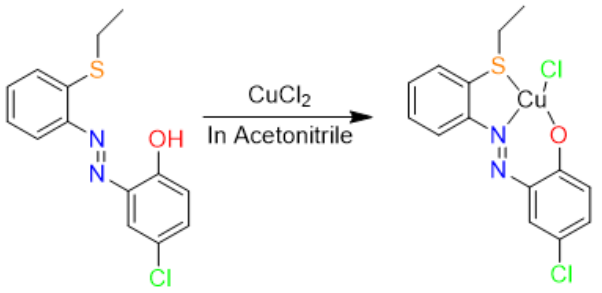


**Scheme 2:** Probable HL with $Cu^{2+}$ complexation mode

The binding mechanism of HL is given in Scheme 2. The stoichiometry of the chemosensor probe and $Cu^{2+}$ is 1 : 1 and it is further confirmed by the Job's plot shown in Fig. 4 and it is further confirmed by HRMS spectra. The HL – $Cu^{2+}$ complex shows a signal at m/z 413.523 in the HRMS spectra. Both the experiments confirm that a strong association occurs between the radii of $Cu^{2+}$ and the cavity space of the chemosensor which results in strong interaction between $Cu^{2+}$ and the coordinating sites of the ligand.

### pH study

The $Cu^{2+}$ sensing by the probe was studied at different pH levels to achieve more extensive results. HEPES buffer solution was used, and the UV-absorption spectra of the chemosensor probe (HL) were examined both in the absence and presence of $Cu^{2+}$ ions. Aqueous solutions of 1 M HCl or 1 M NaOH were employed to adjust the pH.

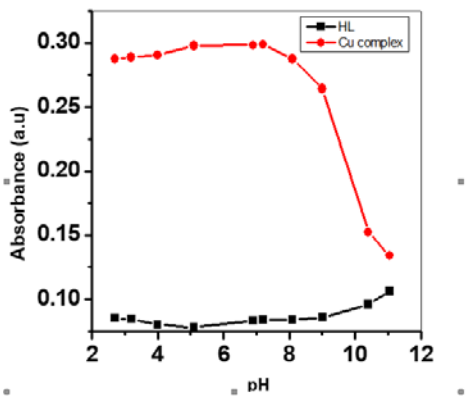


**Figure 5**: Absorbance vs pH plot of chemosensor and chemosensor-$Cu^{2+}$ at 515 nm (10 µM) in $CH_3CN$ *(Source: Roy et al., 2017)*

Spectra shows, the absorption intensity of the chemosensor probe is almost unaffected at different pH condition but it shows a large change of absorption intensity between pH 8- 11 in presence of $Cu^{2+}$ ion. Between the pH 5-8, the probe can form a stable complex with $Cu^{2+}$ ion. The probe has a tendency to combine with proton At very low pH (< 3) and so the probe is less effective in sensing the $Cu^{2+}$ at very low pH. Hence, it is evident that the synthesized probe can sense $Cu^{2+}$ ions within the pH range of 5-8.

**DFT Computational studies for HL-$Cu^{2+}$ complex**

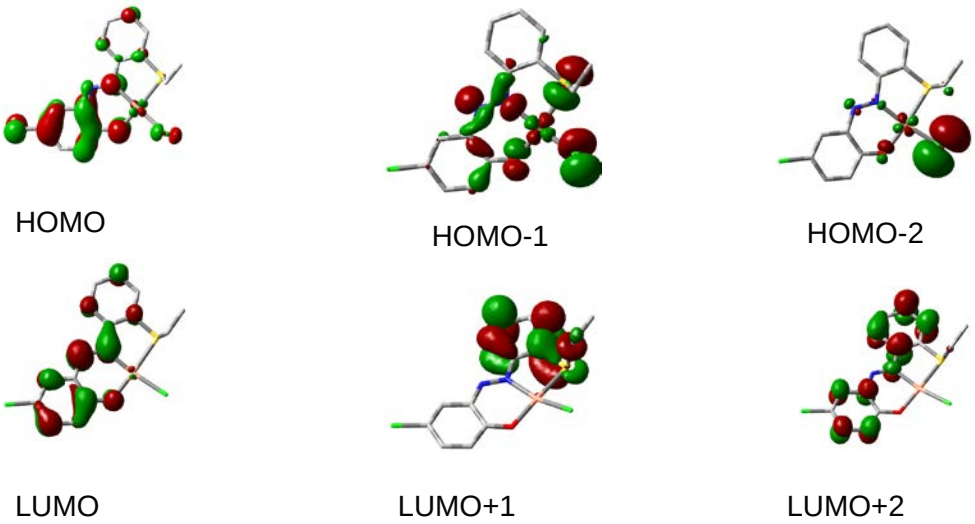


**Figure 6**: Some selected α-spin molecular orbitals of chemosensor $Cu^{2+}$Complex
*(Source: Roy et al., 2017)*

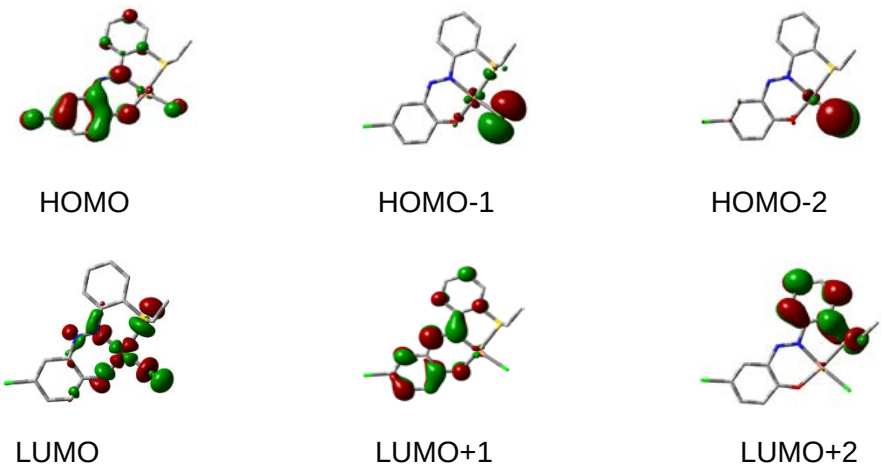


**Figure 7**: Some selected *β*-spin molecular orbitals of chemosensor-$Cu^{2+}$Complex
*(Source: Roy et al., 2017)*

***Table 1:*** *Energy and percentage compositions of some selected α-spin molecular orbitals of chemosensor-$Cu^{2+}$Complex*

| Molecular Orbitals | Energy | Percentage Composition | | |
|---|---|---|---|---|
| | | Cu | Ligand | Cl |
| LUMO+5 | 0.36 | 50 | 50 | 0 |
| LUMO+4 | -0.04 | 42 | 57 | 01 |
| LUMO+3 | -0.24 | 01 | 99 | 0 |
| LUMO+2 | -0.63 | 01 | 99 | 0 |
| LUMO+1 | -1.35 | 03 | 97 | 0 |
| LUMO | -3.12 | 01 | 99 | 0 |
| HOMO | -6.03 | 03 | 93 | 04 |
| HOMO-1 | -6.43 | 12 | 61 | 26 |
| HOMO-2 | -6.73 | 05 | 09 | 87 |
| HOMO-3 | -6.84 | 06 | 09 | 85 |
| HOMO-4 | -7.12 | 01 | 96 | 03 |
| HOMO-5 | -7.49 | 06 | 57 | 38 |
| HOMO-6 | -7.67 | 01 | 97 | 02 |
| HOMO-7 | -8.21 | 01 | 98 | 01 |
| HOMO-8 | -8.48 | 06 | 81 | 13 |
| HOMO-9 | -8.68 | 07 | 93 | 01 |
| HOMO-10 | -8.72 | 0 | 100 | 0 |

***Table 2:*** *Energy and percentage compositions of some selected β-spin molecular orbitals of chemosensor-$Cu^{2+}$Complex*

| Molecular Orbitals | Energy | Percentage Composition | | |
|---|---|---|---|---|
| | | Cu | Ligand | Cl |
| LUMO+5 | -0.03 | 43 | 57 | 01 |
| LUMO+4 | -0.22 | 01 | 99 | 0 |
| LUMO+3 | -0.62 | 01 | 99 | 0 |
| LUMO+2 | -1.34 | 03 | 97 | 0 |
| LUMO+1 | -3.08 | 01 | 99 | 0 |
| LUMO | -3.66 | 47 | 40 | 13 |
| HOMO | -6.02 | 03 | 92 | 05 |
| HOMO-1 | -6.02 | 04 | 07 | 89 |
| HOMO-2 | -6.75 | 06 | 06 | 88 |
| HOMO-3 | -7.04 | 03 | 78 | 19 |
| HOMO-4 | -7.16 | 03 | 83 | 14 |
| HOMO-5 | -7.64 | 01 | 98 | 01 |
| HOMO-6 | -8.14 | 06 | 85 | 10 |

| | | | | |
|---|---|---|---|---|
| HOMO-7 | -8.22 | 03 | 96 | 01 |
| HOMO-8 | -8.49 | 32 | 52 | 17 |
| HOMO-9 | -8.67 | 15 | 77 | 08 |
| HOMO-10 | -8.71 | 02 | 98 | 0 |

HOMO of (α-spin) have a reduced contribution of dπ(Cu) along with a major contribution of π(L). The LUMO (α-spin) has 99% π * (L) character, with a major contribution of π * (N=N). LUMO+1 to LUMO+3 have π * (L) character. The HOMOs of β-spin again have π(L) character, but significant contributions of the dπ(Cu) orbitals have been found in HOMO-8 in comparison with the α-spin occupied molecular orbitals. The LUMO (*β*-spin) has 47% dπ(Cu) character. The LUMO+1 (*β*-spin) to LUMO+4 (*β*-spin) have π * (L) character. In the UV-Vis spectra of the $Cu^{2+}$complex shoulder peak at 410 and 323 nm corresponds to π(L) → π * (L). For the copper (II) complex, the weak bands at 515 nm corresponds to mixed intra-ligand charge transfer (ILCT), π(L) → π * (L), and ligand to metal charge transfer (LMCT), π(L) → dπ(Cu), transitions.

## Conclusion

An azo-phenol moiety-based chemosensor is synthesized and different spectroscopic techniques have been used to confirm its structure. The chemosensor showed a significant colour change from faint yellow to purple, while the chemosensor made a complex with $Cu^{2+}$ but it did not show any significant colour change while studied with other competitive metal ions. Job's plot and mass spectroscopic analysis have been used to predict the 1:1 chemosensor-$Cu^{2+}$ complex formation. pH study shows that the synthesized probe can sense $Cu^{2+}$ ion between the pH range 5-8 . DFT studies have been performed to explain the binding mechanism between the HL and $Cu^{2+}$. Association constant (Ka, $8.94 \times 10^4$ $M^{-1}$) indicates that the synthesized probe has a very high affinity for binding to the $Cu^{2+}$ ion.

## Acknowledgement

The author is grateful to Netaji Nagar Day College and Jadavpur University, India for their encouragement, support and constant help.

## References

Ajayakumar, M. R., Mukhopadhyay, P., Yadav, S., & Ghosh, S. (2010). Single-electron transfer driven cyanide sensing: a new multimodal approach. *Organic Letters*, *12*(11), 2646-2649.

Barone, V., & Cossi, M. (1998). Quantum calculation of molecular energies and energy gradients in solution by a conductor solvent model. *The Journal of Physical Chemistry A*, *102*(11), 1995-2001. https://doi.org/10.1021/jp9716997

Bauernschmitt, R., & Ahlrichs, R. (1996). Treatment of electronic excitations within the adiabatic approximation of time dependent density functional theory. *Chemical Physics Letters*, *256*(4-5), 454-464. https://doi.org/10.1016/0009-2614(96)00440-X

Beck, A. D. (1993). Density-functional thermochemistry. III. The role of exact exchange. *J. Chem. Phys*, *98*(7), 5648-5652. https://doi.org/10.1063/1.464913

Cao, F., Jiao, F., Ma, S., & Dong, D. (2022). Laser-induced breakdown spectroscopy mediated amplification sensor for copper (Ⅱ) ions detection using click chemistry. *Sensors and Actuators B: Chemical*, *371*, 132594. https://doi.org/10.1016/j.snb.2022.132594

Chang, L. W. (Ed.). (2023). *Toxicology of Metals, volume I*. CRC press, USA.

Chen, X., Nam, S. W., Kim, G. H., Song, N., Jeong, Y., Shin, I., ... & Yoon, J. (2010). A near-infrared fluorescent sensor for detection of cyanide in aqueous solution and its application for bioimaging. *Chemical Communications*, *46*(47), 8953-8955. https://doi.org/10.1039/C0CC03398G

Cossi, M., Rega, N., Scalmani, G., & Barone, V. (2003). Energies, structures, and electronic properties of molecules in solution with the C-PCM solvation model. *Journal of Computational Chemistry*, *24*(6), 669-681. https://doi.org/10.1002/jcc.10189

Dalapati, S., Jana, S., Alam, M. A., & Guchhait, N. (2011). Multifunctional fluorescent probe selective for Cu (II) and Fe (III) with dual-mode of binding approach. *Sensors and Actuators B: Chemical*, *160*(1), 1106-1111. https://doi.org/10.1016/j.snb.2011.09.034

Elmagbari, F. M., Hammouda, A. N., Soliman, S. M., EL-Ferjani, R. M., Elagili, F. A., Amer, Y. O. B., ... & Bonomo, R. P. (2024). Solution structure, crystal structure, Hirshfeld surface analysis of copper (II) diamide species as an optical chemical sensor. *Polyhedron*, *256*, 116996. https://doi.org/10.1016/j.poly.2024.116996

Finkel, T., Serrano, M., & Blasco, M. A. (2007). The common biology of cancer and ageing. *Nature*, *448*(7155), 767-774. https://doi.org/10.1038/nature05985

Frisch, M. J. E. A. (2009). gaussian 09, Revision d. 01, Gaussian. *Inc, Wallingford CT*, *201*.

Furche, F., & Ahlrichs, R. (2002). Adiabatic time-dependent density functional methods for excited state properties. *The Journal of Chemical Physics*, *117*(16), 7433-7447. https://doi.org/10.1063/1.1508368

Guo, Z. Q., Chen, W. Q., & Duan, X. M. (2010). Highly selective visual detection of Cu (II) utilizing intramolecular hydrogen bond-stabilized merocyanine in aqueous buffer solution. *Organic Letters*, *12*(10), 2202-2205. https://doi.org/10.1021/ol100381g

Hahn, S. H., Tanner, M. S., Danke, D. M., & Gahl, W. A. (1995). Normal metallothionein synthesis in fibroblasts obtained from children with Indian childhood cirrhosis or copper-associated childhood cirrhosis. *Biochemical and Molecular Medicine*, *54*(2), 142-145. https://doi.org/10.1006/bmme.1995.1021

Hay, P. J., & Wadt, W. R. (1985). An initio effective core potentials for molecular calculations. Potentials for the transition metal Sc to Hg. *The Journal of Chemical Physics*, *82*(1), 270-283.

https://doi.org/10.1016/j.surfin.2024.104301

Kim, B. E., Nevitt, T., & Thiele, D. J. (2008). Mechanisms for copper acquisition, distribution and regulation. *Nature Chemical Biology*, *4*(3), 176-185.

Lee, C., Yang, W., & Parr, R. G. (1988). Development of the Colle-Salvetti correlation-energy formula into a functional of the electron density. *Physical Review B*, *37*(2), 785. https://doi.org/10.1103/PhysRevB.37.785

Linder, M. C., & Hazegh-Azam, M. (1996). Copper biochemistry and molecular biology. *The American Journal of Clinical Nutrition*, *63*(5), 797S-811S. https://doi.org/10.1093/ajcn/63.5.797

Robinson, N. J., & Winge, D. R. (2010). Copper metallochaperones. *Annual Review of Biochemistry*, *79*, 537-562. https://doi.org/10.1146/annurev-biochem-030409-143539

Roy, P., Das, S., Aich, K., Gharami, S., Patra, L., & Mondal, T. K. (2017). A new highly selective and ratiometric chromogenic sensor for $Cu^{2+}$ detection. *Journal of the Indian Chemical Society, 94*, 755-760.

Scalmani, G., Frisch, M. J., Mennucci, B., Tomasi, J., Cammi, R., & Barone, V. (2006). Geometries and properties of excited states in the gas phase and in solution: Theory and application of a time-dependent density functional theory polarizable continuum model. *The Journal of Chemical Physics*, *124*(9). https://doi.org/10.1063/1.2173258

Shang, L., Zhang, L., & Dong, S. (2009). Turn-on fluorescent cyanide sensor based on copper ion-modified CdTe quantum dots. *Analyst*, *134*(1), 107-113. https://doi.org/10.1039/B812458B

Stratmann, R. E., Scuseria, G. E., & Frisch, M. J. (1998). An efficient implementation of time-dependent density-functional theory for the calculation of excitation energies of large molecules. *The Journal of Chemical Physics*, *109*(19), 8218-8224. https://doi.org/10.1063/1.477483

Trevino, K. M., Wagner, C. R., Tamura, E. K., Garcia, J., & Louie, A. Y. (2023). Small molecule sensors for the colorimetric detection of Copper (II): A review of the literature from 2010 to 2022. *Dyes and Pigments*, *214*, 110881. https://doi.org/10.1016/j.dyepig.2022.110881

Veedu, A. P., Kumar, S. K., Kuppusamy, S., Mohan, A. M., & Deivasigamani, P. (2024). Solid-state real-time colorimetric sensing of ultra-trace copper ions using aqueous compatible chromatic probe imbued porous polymer monolithic sensor. *Surfaces and Interfaces*, *48*, 104301. https://doi.org/10.1016/j.surfin.2024.104301

Vulpe, C., Levinson, B., Whitney, S., Packman, S., & Gitschier, J. (1993). Isolation of a candidate gene for Menkes disease and evidence that it encodes a copper–transporting ATPase. *Nature Genetics*, *3*(1), 7-13. https://doi.org/10.1038/ng0193-7

Wadt, W. R., & Hay, P. J. (1985). Ab initio effective core potentials for molecular calculations. Potentials for main group elements Na to Bi. *The Journal of Chemical Physics*, *82*(1), 284-298.

Zou, Q., Li, X., Zhang, J., Zhou, J., Sun, B., & Tian, H. (2012). Unsymmetrical diarylethenes as molecular keypad locks with tunable photochromism and fluorescence via $Cu^{2+}$ and $CN^-$ coordinations. *Chemical Communications*, *48*(15), 2095-2097. https://doi.org/10.1039/C2CC16942H